Revealing light momentum in dielectric media through standing-wave radiation pressure

Gopal Verma [1,2,*] Vinod Kumar [3] and Wei Li [1,†]

[1]*GPL Photonics Laboratory, State Key Laboratory of Luminescence and Applications, Changchun Institute of Optics, Fine Mechanics and Physics, Chinese Academy of Sciences, Changchun, Jilin 130033, People's Republic of China*

[2]*Gopal Photonics Research Laboratory (GPRL) Basti, Pandari Mishra, Amari Bazar, Uttar Pradesh 272155, India*

[3]*Department of Physics, The University of the West Indies, St. Augustine, 330912 Trinidad and Tobago*

(Received 24 May 2023; revised 4 August 2023; accepted 3 October 2023; published 26 October 2023)

Air-water interface deformation has been used as a testbed to resolve the momentum of light debate (Abraham-Minkowski) inside the dielectric medium, but to date, experiments or theory which have resolved this debate precisely are lacking. Here, we present the experimental observation of both momenta in a single setup. The model employed in interpreting our experimental results suggests that the total momentum associated with light inside a dielectric is represented by the mean value of the Abraham and Minkowski momenta, which is $\frac{1}{2}(n + 1/n)\hbar\omega/c$. We used a clean and relatively simple pump-probe-type setup to investigate the light momentum inside the dielectric medium. Using a pump beam, we generate a standing wave, formed due to an incident and reflected pump beam in a water drop, placed on a partially metallic coated prism. A weak red probe laser beam was used to detect the nanoscale height variation of the air-water interface, where natural evaporation enabled us to measure the radiation pressure variations (spacing between the node and antinodes, $\lambda/2n$) in the standing wave. Our results clearly depict the dependence of radiation pressure upon the phase of the incident and reflected light. We also performed numerical simulations in realistic experimental settings and found good agreement with the experimental results, and offer potential applications in microfluidics and optofluidics.

DOI: 10.1103/PhysRevA.108.043514

I. INTRODUCTION

The formulation of two different yet fundamental momenta [1,2], laid down by Abraham and Minkowski for light in a refractive medium, has fueled a debate for over a century. Theoretically, Abraham and Minkowski's momenta were identified as kinetic and canonical momenta, respectively [3–15]. However, it has been left to experiments to decide which one would manifest for a given situation [16–21]. In this regard, Jones-Richards-Leslie (JRL) [22–24] provided the first experimental evidence that the optical pressure on submerged mirrors is proportional to the refractive index of the liquid (n), in favor of the Minkowski momentum. General expressions for the electromagnetic force, applicable to inhomogeneous, anisotropic, and dispersive media, were also developed in Ref. [9]. It was shown that the Abraham momentum could explain the dependence of the radiation pressure on the refractive index in the experiments of Jones and Leslie [22–24]. Furthermore, in Refs. [15,25–27], a covariant theory of light propagation in a medium reveals the transfer of a measurable mass carried by a mass-density wave.

This dilemma has recently been revisited in several studies [15,25–32]. The analysis suggests that the measured radiation pressure (or light momentum) inside a dielectric medium would depend on the chosen value of the phase shift of the reflected wave (ϕ) for the submerged mirror, and could favor a photon momentum anywhere in the range between the Abraham and Minkowski values. Previous studies [22–24] measured the deflection of a mirror submerged in various liquids, but neglected the standing-wave effects. However, it is necessary to take into account the radiation pressure felt by the liquid in its interaction with the standing-wave fringes to balance between the free-space momenta of the incident and reflected beams and the force experienced by the mirror [28,29].

There are two major bottlenecks to experimentally observing the effect of standing waves on radiation pressure. First and foremost is that the technique used must be capable of observing surface deformations between a node and an antinode of the standing wave. The surface deformations caused by radiation pressure produced by the refractive-index discontinuity ($\Pi_{\Delta n}$) and the standing wave ($\Pi_{\rm sw}$) have a small difference in magnitude (<10 nm). Therefore, the technique must be precise enough to differentiate between the two. The second challenge is that a system is needed where the height of the dielectric medium can be smoothly varied at the nanoscale.

In this paper, we investigated light momentum in a dielectric medium using an interferometer-equipped pump-probe setup. A standing wave was generated in a water drop on a partially metallic-coated prism, and nanoscale surface deformations were measured using a weak red laser beam through interferometry. Our modified liquid drop interferometer (LDI) experiment demonstrated the phase-dependent deformation of the air-water interface due to the standing wave and refractive-index discontinuity, with a precise distinction between the two. Our results showed that the interface deformation varied according to the phase-dependent pressure of the standing wave, and the total momentum transfer to the liquid was the mean of the Abraham and Minkowski forms of momentum.

*gopal@gprl.org.in
†weili1@ciomp.ac.cn

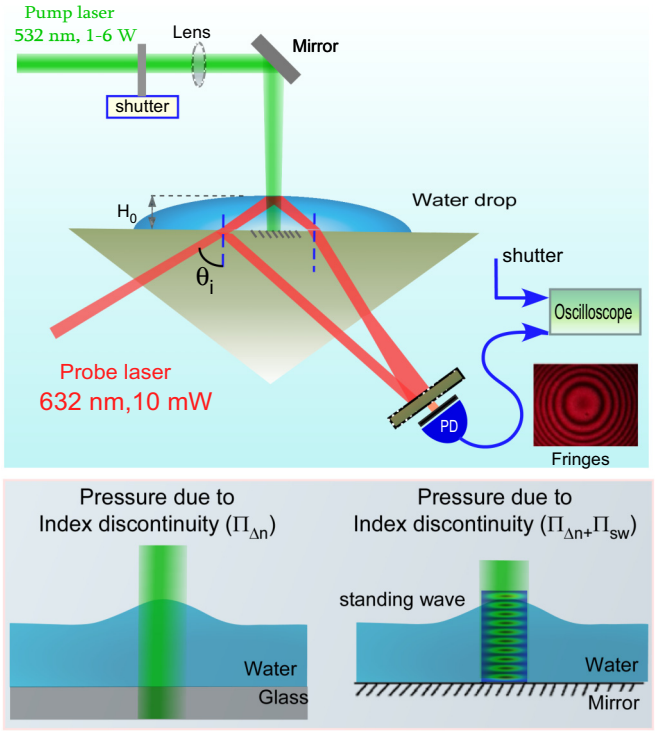

FIG. 1. Schematic of the experimental setup. A continuous wave (CW) green pump beam ($\lambda = 532$ nm) shined at incident angle θ_i is used to locally deform the fluid drop (initial height H_0). A collimated He-Ne laser produced a dynamic interference pattern from a fluid drop. The photodiode (PD) measured the intensity of the central fringe. The radius of the drop was ~2–5 mm, $T = 25 \pm 1\,^{\circ}$C, 50% relative humidity (RH).

Our simple yet sensitive method analyzed the interplay between light momentum and fluid dynamics [33], paving the way for potential optofluidic applications.

II. EXPERIMENTAL METHOD AND RESULTS

The interferometric pump-probe setup used in the experiment is shown in Fig. 1. A water droplet was placed on a prism with a partial metallic coating ($R > 97\%$), which allowed for the creation of a standing wave by a normally incident pump laser beam. A He-Ne probe laser was used to generate interferometric fringes from the reflections of the glass-water and water-air interfaces. The probe beam was coupled from below the prism to avoid a large mismatch of the reflection coefficient at the air-water and mirror-water interfaces. Analysis of the interference fringe pattern with the baseline of the natural evaporation of water enabled the measurement of the surface height variation with nanometer sensitivity (δH_0) due to the optical force.

A. Water drop on glass prism

First, we performed a requisite test with a planar glass prism (without any metallic coating) to demonstrate the measurement of light momentum where the effects of standing-wave or phase changes are not observable. For this we shined a pump laser with a wavelength and beam waist ($\lambda = 532$ nm, $w_e = 200$ μm) normally at the air-water (AW) interface of a large water droplet ($V = 50$ μl, $r_0 = 5$ mm, base radius of the droplet).

For a laser beam normally incident from free space (air) onto a flat surface of a dielectric (water) liquid, after a few nanoseconds, the volume contribution of the electrostriction is canceled out by its surface contribution [18]. The surface motion timescale is much longer than this initial transient and the surface deformation is described by that due to the Minkowski-Abraham term as well as those due to gravity and surface tension [18,19,34]. The overall radiation pressure that elevates the surface of the liquid is give by $\Pi_{\Delta n} = -2I(r)(n_l - 1)/[c(n_l + 1)]$.

We probed the deformation height using a low-power red laser ($P_0 = 10$ mW, $w_p = 650$ μm) as the probe beam. A comparable reflectivity of light from the AW and glass-water (GW) interfaces and high-contrast circular fringes are made by the interferometric probe beam. We analyzed these fringes to obtain the surface deformation with direction. The disappearance of one central fringe corresponded to a $\lambda/4n_l = 119$ nm change in the optical path length in the drop and gave the self-calibration. The natural evaporation of water continuously reduced the droplet thickness. This resulted in dynamic interference fringes and provided an oscillatory curve of intensity [$I_p(t)$, the red curve in Fig. 2] when the central fringe was tracked. By resolving the central fringe intensity between consecutive maxima and minima, we achieved a precision of <2 nm in the surface deformation measurement. The continuous decline in water height also served as a reference to determine the direction (dimple/bump) of the deformation [19,21,33,35]. We also controlled the evaporation rate or ($\delta H_0/\delta t$) by a partial enclosure to achieve stable steady-state evaporation.

Any actuation of the drop interface by the radiation pressure changes the optical path, and modifies the intensity of the central fringe which, as such, contains the temporal signature of the induced deformation. An example of a temporal variation of the central intensity of the fringe pattern in the absence and presence of radiation pressure is illustrated in Figs. 2(a) and 2(c) for pure water. When the pump beam is turned on with the shutter (lower green signal in Fig. 2), the optical path difference between the probe beam reflection at AW and the GW interface suddenly changes and modifies the central intensity of $I_p(t)$ of the fringe. The subtraction of the sine modulation eventually isolated the response induced by the switching on/off of the pump beam (as shown in the lower panel in Fig. 2). Enlargement of the opening/closing duration of the shutter [Fig. 2(c)] showed that the AW interface adiabatically followed the pump beam as shown by approximately the same rise/fall times for the green curves. This unambiguously demonstrated that the pump beam induced an increase in the height of the AW interface, resulting in an outward bulge towards and supporting Minkowski's form of momentum [18,21,35].

B. Water drop on partially silvered glass prism

"What would happen if we placed the water drop on a metallic mirror surface?" To investigate this, we made some modifications to the LDI technique [36] in order to avoid

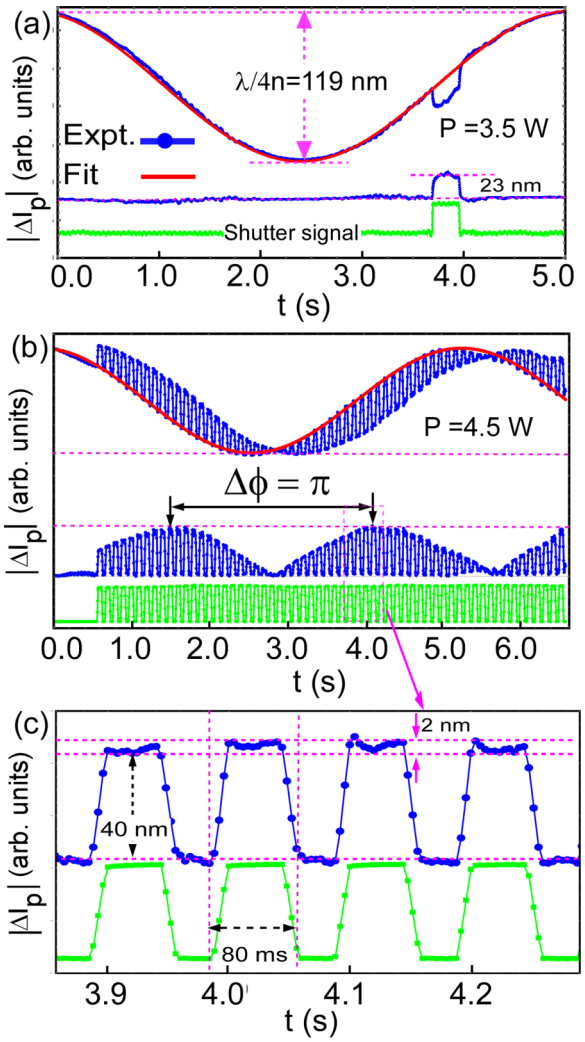

FIG. 2. (a), (b) Probe intensity $I(t)$ in terms of nanometer vs time. The solid red line is a $I_p(t)\cos^2[\alpha_0 d(t)]$ fit to the simulated data (blue) corresponding to natural evaporation and pump beam excitation. (c) Zoom near the maximum deformation height.

the strong Fresnel reflection from the water-metallic mirror interface. For this, we used a partially silvered (2 mm circular radius or rectangular strip) glass prism with a highly reflective (>99%) mirror. We shined a pump laser beam normally at the water droplet placed on the silvered prism, and due to the refractive-index discontinuity, radiation pressure $\Pi_{\Delta n}$ was exerted at the AW interface. Additionally, the high reflectivity of the mirror and standing wave were considered to be formed by the interference between the incident and reflected waves from the mirror (see Fig. 1). The radiation pressure exerted by the standing wave at the mirror surface can be computed using the Lorentz force density [28]. Considering that neither the liquid nor the metallic reflector absorb the light, the radiation pressure on the mirror given is by [28]

$$\Pi^m_{\rm sw} = [n^2/(\sin^2\phi + n^2\cos^2\phi)](I/c), \tag{1}$$

where $\phi = 2\pi n_l H_0(t)/\lambda_0$ is the single-path phase shift through the liquid column, $I(=\epsilon_0 cnE_0^2)$ is the light intensity, and c is the speed of light. Thus the radiation pressure on the immersed mirror was found to be greater than or equal to that experienced by the same mirror in free space, namely, I/c.

Considering the momentum balance between the free space of the incident and reflected beams and the force experienced by the submerged mirror, one must take into account the radiation pressure felt by the liquid in its interaction with the standing-wave fringes between the mirror and the surface of the liquid [28,29]. The volumetric force on a liquid column calculated as $F_z(z) = (2\pi n_l/\lambda_0)\left[\frac{I(n_l^2-1)\sin^2\phi}{c(\sin^2\phi+n_l^2\cos^2\phi)}\right]\sin[4\pi n_l(z-H_0(t))/\lambda_0]$. This volumetric force density, which varies sinusoidally between positive and negative values, averages out to zero within each fringe of the standing wave. When integrated from $z=0$ to $H_0(t)$, it yields the force per unit cross-sectional area (radiation pressure) of the liquid column as follows [28,29]:

$$\Pi^l_{\rm sw} = -\frac{I\left(n_l^2-1\right)\sin^2\phi}{c\left(\sin^2\phi + n_l^2\cos^2\phi\right)}. \tag{2}$$

For this scenario, the total radiation pressure exerted on the AW interface is given by $\Pi_z = \Pi_{\Delta n} + \Pi^l_{\rm sw}$. This pressure depends on the position of the AW interface between the nodes and antinodes of the standing wave. If the height $H_0(t)$ of the drop happens to be an integer multiple of $\lambda/2n_l$, the values of phase $\phi = 2\pi n_l H_0(t)/\lambda = \pi$ and pressure $\Pi^l_{\rm sw} = 0$. However, if $H_0(t)$ differs by $\lambda/4n_l = 100$ nm ($\lambda = 532$ nm, $n_l = 1.33$), pressure $\Pi^l_{\rm sw}$ acquires its maximum value. Intriguingly, one can see the difference in deformation heights (<10 nm) of the AW interface at opposite phases of the sinusoidal probe signal, This is due to the resultant radiation pressure variation and the standing-wave pressure [see Figs. 3(a)–3(c)]. This observation was only made possible because of the high sensitivity and self-calibration nature of the technique used.

We also numerically modeled the effects of resultant radiation pressure Π_z on the AW interface using a finite-element analysis (FEA). We used the wave optics module to generate the standing wave and calculated the stress at the AW and water-mirror (MW) interface (see Fig. 4). The effects of the radiation pressure on the surface displacement were calculated by solving the Navier-Stokes equation with appropriated boundary conditions. Here,

$\rho\frac{dv}{dt} + \rho(v\cdot\nabla)v = -\nabla P + \eta\nabla^2 v + F$, where v describes the flow velocity, P is the pressure, ρ is the fluid density, μ is the dynamic viscosity, and $F = \rho g$ with $g = 9.8$ m/s^2. The model was built in the two-dimensional (2D) axisymmetric geometry. The external pressure and surface tension were made to act on the AW interface. Free-surface and no-slip boundary conditions were applied at the liquid and substrate interfaces $v_x(z=0) = 0$. A realistic sample geometry was considered (see the inset of Fig. 4, $R = 20$ mm and $h_0 = 0.1$–1 mm).

Figures 4(a) and 4(b) demonstrate that the AW interface's bulge height varies under applied total stress $\Pi_z = \Pi_{\Delta n} + \Pi_{\rm sw}$, as the drop height changes, causing the nodes to change into antinodes of the standing wave at the AW interface. The minimum bulge height corresponds to the height induced by the pressure $\Pi_{\Delta n}$ alone, where $\Pi_{\rm sw} = 0$. On the other hand, the maximum height is observed when $\Pi_{\rm sw}$ reaches its maximum value, which is approximately 7 nm for a 3.5 W laser power (experimental), greater than the

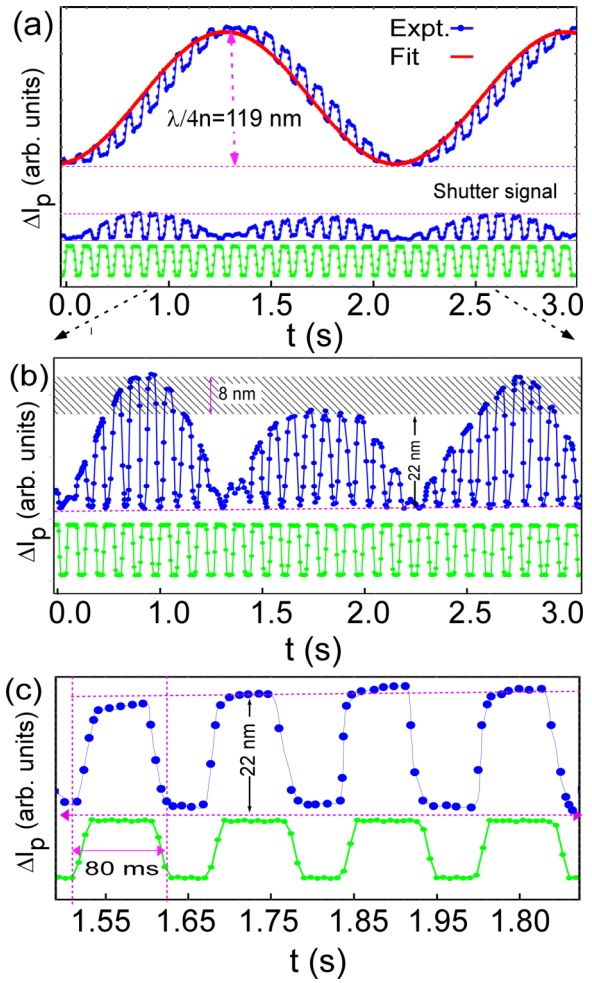

FIG. 3. (a), (b) Probe intensity $I(t)$ in terms of nanometer vs time for pump on-off cycles for $P_0 = 3.5$ W. The solid red line is a $I_0 \cos^2[\alpha_0 H_0(t)(t)]$ fit to the data (blue) corresponding to natural evaporation. (c) Zoom of (b).

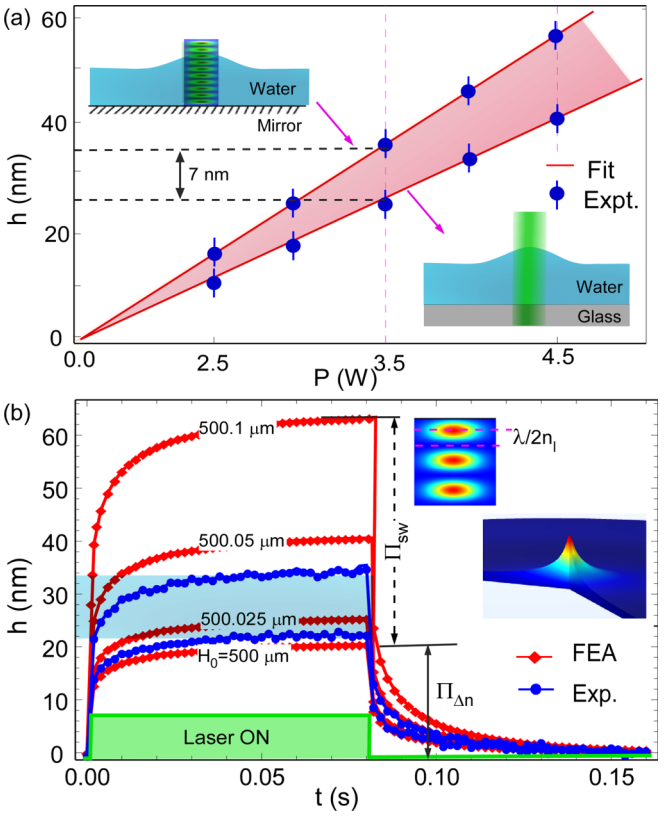

FIG. 4. (a) Power dependence of bulge height of the AW (under total stress, $\Pi_z = \Pi_{\Delta n} + \Pi_{sw}$ acting on the AW interface; $P = 3.5$ W, $w_e = 200$ μm) interface cases where maximum and minimum height correspond to the standing-wave node and antinode at the AW interface. (a) Power dependence difference in bulge height (nodes to antinodes). (b) FEA simulation and experimental data (in blue dots and shaded by a light blue rectangle).

minimum height. To further ensure accuracy, we performed the experiment multiple times, systematically varying the power levels each time. Each power level measurement was based on an average of five shots of the same shutter opening, thereby minimizing the impact of potential fluctuations. As a result, we confidently observed a consistent linear trend: The bulge height increased proportionally with the increase in power level [Fig. 4(a)]. Specifically, at 4.5 W, the measured bulge height was approximately 12 nm. This robust and reproducible relationship between power and bulge height reinforces the reliability of our findings and provides valuable insights into the behavior of the system under different power conditions.

Figure 4(b) presents a comparison between the finite-element analysis (FEA) results and the corresponding experimental data (shown in blue). A notable observation is that the FEA results show a difference of approximately 40 nm between the maximum and minimum heights (due to the contribution of the standing-wave pressure). In contrast, the experimental data demonstrate a much smaller difference of about 7 nm for a laser power of 3.5 W. The difference mainly arises due to the light laser source, which is typically not perfectly monochromatic in practical experiments. In such cases, the radiation pressure is estimated by averaging the force F_z from Eq. (1) over the light source's bandwidth. Assuming an equal likelihood for all values of ϕ, the averaged coefficient of $\varepsilon_0 E_0^2$ in Eq. (1) is found to be equal to n (Minkowski form of momentum), precisely matching the results obtained in many experiments [22–24]. However, in an ideal case (as we considered in our FEA calculation) for an essentially monochromatic beam of light and a perfect reflector it should be about 60 nm. But, in practice, this is not easily attainable, because under such circumstances the bulge height decreases due to less momentum transfer [28].

Previous pump-probe experiments with fluid systems, such as those conducted in Refs. [3,18,21,34,35], reported an outward bump on the AW interface, indicating the uniqueness of the Minkowski form of momentum. However, both CW and pulse lasers were used with a vast range of parameters, yet the mean momentum $\frac{1}{2}(n + 1/n)\hbar\omega/c$ was not observed in all experiments. We provide two plausible explanations for this discrepancy. First, in Refs. [3,18,34], the water sample was kept in a glass cell or glass prism with a small reflection coefficient, which resulted in a very small standing-wave pressure even at normal incidence, as observed in our Fig. 2. Second, we always observed nanoscale bumps with varying

heights due to phase-dependent standing-wave radiation pressure, which induced radiation pressure at the AW interface in the form of a nanobulge, making it seem that only the Minkowski form of momentum appeared. However, with a nanoscale-sensitive technique ($\Delta h < 10$ nm), it is possible to observe that the AW interface deformation follows the mean momentum.

The mean value of the Abraham and Minkowski momenta, $\frac{1}{2}(n + 1/n)\hbar\omega/c$, being greater than the vacuum photon momentum, can be explained by the fact that the photon exerts a pulling force on the water upon entering it (see Fig. 2). Our observation revealed a deformation height difference of about 7 nm between standing-wave nodes and antinodes, which required a precision of measuring the AW water interface height change within $\delta H_0 = 100$ nm. Lastly, we discussed the role of electrostriction in the results, which is important as it is a very timely topic as indicated by the two publications [37–39]. The presence of electrostrictive force introduces compressibility effects in the liquid. It is anticipated that the time required for pressure equilibrium to be established in the water would be comparable to the time taken for sound to travel across the probed volume (with a radius w_p). Taking into account the finite excitation beam width w_e, the acoustic waves would require approximately 560 ns ($w_p = 650$ μm, $w_e = 600$ μm, and sound velocity in water $v_s = 1500$ m/s) to traverse this distance. This observation is in agreement with Brevik's analysis [40] of the Ashkin-Dziedzic experiment [3], where the outward bulge of the free surface of water illuminated by a pulsed laser was studied. However, in our experiment, we employed a continuous-wave laser with a transient time of approximately 10 μs ($\approx 3\eta w_e/\gamma$), where η and γ represent the viscosity and surface tension of water, respectively. This transient time is significantly larger than the 560 ns timescale associated with electrostriction. As a result, the contribution of electrostriction in our results is negligible, allowing us to focus specifically on the influence of standing-wave radiation pressure on the deformed AW interface height.

III. CONCLUSION

In conclusion, our experiment provided a clear distinction between the phase-dependent deformation of the air-water interface due to the pressure of the standing wave. Our observations demonstrated that interface deformation varied with pressure changes within the standing wave. We leaned towards adopting the mean of the Abraham and Minkowski momentum formalism $\frac{1}{2}(n + 1/n)\hbar\omega/c$, as predicted in Refs. [28,29], which finds support in the Doppler shift of light reflected from a moving mirror [31]. This approach fundamentally differs from the Lorentz force but leads to identical conclusions. However, various models [9,24,28,39] provide explanations for the outcomes observed with submerged mirrors. Consequently, it becomes evident that reaching a definitive conclusion regarding the precise value of photon momentum is not feasible, as it profoundly relies on the underlying model. Instead, this determination remains highly model dependent. However, our result is valuable in measuring light momentum inside dielectric media and sheds light on the unique nature of standing waves in fundamental force measurements. Our findings have potential applications in optofluidics, fluid droplets, reconfigurable lenses, and investigating the interplay between fluid dynamics and light momentum. [33,41–43].

ACKNOWLEDGMENTS

We thank J. P. Delville for their insightful discussions and suggestions. This work was supported by the National Natural Science Foundation of China (Grants No. 62134009 and No. 62121005).

[1] H. Minkowski, Die grundgleichungen für die elektromagnetischen vorgänge in bewegten körpern, Nachr. Ges. Wiss. Gottingen, Math.-Phys. Kl. **1908**, 53 (1908).
[2] M. Abraham, Zur elektrodynamik bewegter körper, Rend. Circ. Matem. Palermo **28**, 1 (1909).
[3] A. Ashkin and J. M. Dziedzic, Radiation pressure on a free liquid surface, Phys. Rev. Lett. **30**, 139 (1973).
[4] G. K. Campbell, A. E. Leanhardt, J. Mun, M. Boyd, E. W. Streed, W. Ketterle, and D. E. Pritchard, Photon recoil momentum in dispersive media, Phys. Rev. Lett. **94**, 170403 (2005).
[5] R. N. C. Pfeifer, T. A. Nieminen, N. R. Heckenberg, and H. Rubinsztein-Dunlop, Colloquium: Momentum of an electromagnetic wave in dielectric media, Rev. Mod. Phys. **79**, 1197 (2007).
[6] R. Peierls, The momentum of light in a refracting medium, Proc. R. Soc. London, Ser. A **347**, 475 (1976).
[7] S. M. Barnett, Resolution of the Abraham-Minkowski dilemma, Phys. Rev. Lett. **104**, 070401 (2010).
[8] C. Baxter and R. Loudon, Radiation pressure and the photon momentum in dielectrics, J. Mod. Opt. **57**, 830 (2010).
[9] K. J. Webb, Dependence of the radiation pressure on the background refractive index, Phys. Rev. Lett. **111**, 043602 (2013).
[10] U. Leonhardt, Optics: Momentum in an uncertain light, Nature (London) **444**, 823 (2006).
[11] D. Pile, Fundamental optics: Momentum debate, Nat. Photon. **9**, 418 (2006).
[12] N. L. Balazs, The energy-momentum tensor of the electromagnetic field inside matter, Phys. Rev. **91**, 408 (1953).
[13] W. Shockley, Hidden linear momentum, Phys. Rev. Lett. **20**, 343 (1968).
[14] M. Bethune-Waddell and K. J. Chau, Simulations of radiation pressure experiments narrow down the energy and momentum of light in matter, Rep. Prog. Phys. **78**, 122401 (2015).
[15] M. Partanen, T. Häyrynen, J. Oksanen, and J. Tulkki, Photon momentum and optical forces in cavities, Proc. SPIE **9742**, 974217 (2016).
[16] C.-W. Qiu *et al.*, Photon momentum transfer in inhomogeneous dielectric mixtures and induced tractor beams, Light: Sci. Appl. **4**, e278 (2015).
[17] G. B. Walker and D. G. Lahoz, Experimental observation of abraham force in a dielectric, Nature (London) **253**, 339 (1975).

[18] N. G. C. Astrath *et al.*, Unravelling the effects of radiation forces in water, Nat. Commun. **5**, 4363 (2014).
[19] G. Verma and K. P. Singh, Universal long-range nanometric bending of water by light, Phys. Rev. Lett. **115**, 143902 (2015).
[20] L. Zhang, W. She, N. Peng, and U. Leonhardt, Experimental evidence for Abraham pressure of light, New J. Phys. **17**, 053035 (2015).
[21] G. Verma, K. Chaudhary, and K. P. Singh, Nanomechanical effects of light unveil photons momentum in medium, Sci. Rep. **7**, 42554 (2017).
[22] R. V. Jones, Radiation pressure in a refracting medium, Nature (London) **167**, 439 (1951).
[23] R. V. Jones and J. C. S. Richards, The pressure of radiation in a refracting medium, Proc. R. Soc. London, Ser. A **221**, 480 (1954).
[24] R. V. Jones and B. Leslie, The measurement of optical radiation pressure in dispersive media, Proc. R. Soc. London, Ser. A **360**, 347 (1978).
[25] M. Partanen, T. Häyrynen, J. Oksanen, and J. Tulkki, Photon mass drag and the momentum of light in a medium, Phys. Rev. A **95**, 063850 (2017).
[26] M. Partanen and J. Tulkki, Lorentz covariance of the mass-polariton theory of light, Phys. Rev. A **99**, 033852 (2019).
[27] M. Partanen and J. Tulkki, Lagrangian dynamics of the coupled field-medium state of light, New J. Phys. **21**, 073062 (2019).
[28] M. Mansuripur, Radiation pressure and the linear momentum of the electromagnetic field, Opt. Express **12**, 5375 (2004).
[29] M. Mansuripur, Radiation pressure on submerged mirrors: Implications for the momentum of light in dielectric media, Opt. Express **15**, 2677 (2007).
[30] M. Mansuripur and A. R. Zakharian, Radiation pressure on a submerged absorptive partial reflector deduced from the doppler shift, Phys. Rev. A **86**, 013841 (2012).
[31] M. Mansuripur, Deducing radiation pressure on a submerged mirror from the Doppler shift, Phys. Rev. A **85**, 023807 (2012).
[32] B. A. Kemp and T. M. Grzegorczyk, The observable pressure of light in dielectric fluids, Opt. Lett. **36**, 493 (2011).
[33] G. Verma, G. Yadav, and W. Li, Thin-film dynamics unveils interplay between light momentum and fluid mechanics, Opt. Lett. **48**, 123 (2023).
[34] A. Casner and J.-P. Delville, Laser-induced hydrodynamic instability of fluid interfaces, Phys. Rev. Lett. **90**, 144503 (2003).
[35] G. Verma, H. Chesneau, H. Chraibi, U. Delabre, R. Wunenburger, and J.-P. Delville, Contactless thin-film rheology unveiled by laser-induced nanoscale interface dynamics, Soft Matter **16**, 7904 (2020).
[36] G. Verma and K. P. Singh, Time-resolved interference unveils nanoscale surface dynamics in evaporating sessile droplet, Appl. Phys. Lett. **104**, 244106 (2014).
[37] N. G. C. Astrath, G. A. S. Flizikowski, B. Anghinoni *et al.*, Unveiling bulk and surface radiation forces in a dielectric liquid, Light: Sci. Appl. **11**, 103 (2022).
[38] M. Partanen, B. Anghinoni, N. G. C. Astrath, and J. Tulkki, Time-dependent theory of optical electro- and magnetostriction, Phys. Rev. A **107**, 023525 (2023).
[39] B. Anghinoni, M. Partanen, and N. G. C. Astrath, The microscopic ampère formulation for the electromagnetic force density in linear dielectrics, arXiv:2304.06784.
[40] I. Brevik, Experiments in phenomenological electrodynamics and the electromagnetic energy-momentum tensor, Phys. Rep. **52**, 133 (1979).
[41] D. Psaltis, S. R. Quake, and C. Yang, Developing optofluidic technology through the fusion of microfluidics and optics, Nature (London) **442**, 381 (2006).
[42] C. Monat, P. Domachuk, and B. J. Eggleton, Integrated optofluidics: A new river of light, Nat. Photon. **1**, 106 (2007).
[43] G. Verma, G. Yadav, C. Saraj, L. Li, N. Miljkovic, J. Delville, and W. Li, A versatile interferometric technique for probing the thermophysical properties of complex fluids, Light: Sci. Appl. **11**, 115 (2022).